Journal of Engineering Science and Technology
Vol. 18, No. 6 (2023) 3140 - 3154

EVALUATION OF SUBSTRATE MATERIALS AND MASS STRUCTURE ON PIEZOELECTRIC CANTILEVER BASED ENERGY HARVESTER

FAHMIDUL HUQ SYED, LI WAH THONG*, YEE KIT CHAN

Faculty of Engineering and Technology, Multimedia University, Melaka Campus, Jalan Ayer Keroh Lama, 75450, Bukit Beruang, Melaka, Malaysia
*Corresponding Author: lwthong@mmu.edu.my

Abstract

As the world progresses towards sustainable energy, piezoelectric energy harvesting system secures an escalating interest to shape up the idea of energy harvesting for application and devices that require small fraction of power. The current shortcoming of piezoelectricity is its narrow operating frequency bandwidth. This leads to it being only effective in limited circumstances. The purpose of this research is to identify the fundamental factors contributing to achieving a more stable and wide operating frequency bandwidth without applying any external medium to the system. COMSOL Multiphysics was applied to simulate the cantilever beam by changing the configuration of the system, such as size, shape, and the material of the tip mass, within a range of 0-300 Hz. From the simulations results, Tungsten outperforms all the other materials in every tested configuration and aluminium produces the least magnitude of voltage and power. The rest of the materials show sufficient outputs, while some of the materials display stable value at their peak for a few consequent frequencies, including aluminium. The results would help explore conditions that may lead to the enhancement of the output for further use in various devices and applications.

Keywords: Cantilever beam, Energy harvesting, Piezoelectricity, Substrate materials, Vibration.

1. Introduction

The utilization of natural vibrations for energy harvesting technologies has emerged as a highly researched area in recent areas. Vibrational sources are abundant in various aspects of our daily lives, including large infrastructures such as bridges, buildings, roads, and vehicles. Given the accessibility of vibrational energy in the surrounding environment, there has been significant interest in harvesting and converting it into usable power for small electric devices. Researchers have explored and implemented various methods for vibration-based energy harvesting techniques, which can broadly be categorized into four transduction techniques: piezoelectric, electromagnetic, electrostatic, and triboelectric methods [1-3].

Over the years, numerous trials of developing vibration-based piezoelectric harvesters have been done by many researchers. Since these analytical models can speculate the output result and assess the effectiveness of electromechanical energy conversion structures, they can provide guidance to optimize the design of piezoelectric generators. The cantilevered piezoelectric beam harvester stands out as the most efficient and uncomplicated approach among these models for generating substantial electrical energy from a consistent mechanical excitation [4].

In traditional piezoelectric vibration energy harvesters, a cantilever beam with a tip mass is commonly used to enhance power output and lower the operating frequency. However, a significant challenge in resonant vibration energy harvesters is their optimal performance is restricted to a narrow bandwidth centred around the fundamental resonant frequency. Even a slight deviation of the excitation frequency from the resonance condition can lead to a drastic reduction in power output [5]. To address this limitation, a novel piezoelectric harvester design using S-shaped wavy beam was introduced [6]. The dynamic electromechanical coupling response of this new harvester was examined through numerical simulations and experimental validation, demonstrating that the combined bending and torsional motion of the proposed harvester can enhance power generation. In [7] a piezoelectric energy harvester with a multi-mode dynamic magnifier. This harvester utilized a multi-mode intermediate beam with a tip mass. Another dynamic magnifier was proposed in [8] to power output and broaden the bandwidth. A distributed-parameter model of cantilevered piezoelectric beam energy harvester that incorporated a tip mass and a dynamic magnifier was derived in [9]. By carefully selecting and implementing the design parameters of the magnifier, the harvested power output could significantly be enhanced. Additionally, the effective bandwidth of the harvester was improved. However, in all these proposed models, the size of the tip mass offset was overlooked.

However, in recent years, piezoelectric array harvester has been modelled and simulated in COMSOL Multiphysics in [10], setting the tip masses in an inclination set up to enhance the power generation and has been validate with previously obtained experimental data. Different shapes of harvester have been tested for optimized outcome in [11]. A frequency tunning mechanism within sliding masses was developed and implemented in [12].

In energy harvesting design consisting of cantilever beams, the beams are typically categorized into two configurations known as the unimorph and bimorph cantilever beams. The bimorph piezoelectric cantilever beam consists of two layers, one of which is a piezoelectric element, and the other is a non- piezoelectric element

known as the 'substrate layer'. The top and bottom surfaces of the piezoelectric element are equipped with electrodes to collect the charges generated. Adding extra mass to the system, in the form of a tip/proof mass at the free end of the beam, can decrease the resonance frequency. The use of piezoelectric-based design is advantageous due to its low voltage and current requirements. Piezoelectric materials have bi-directional effects, which makes them useful for a wide range of applications such as sensors and actuators. They can also generate electrical energy from the impact of footsteps or other form of motion, which can power electronic devices [13]. In contrast to bimorph cantilever beams, the unimorph system does not involve squeezing the substrate material between two layers of piezoelectric materials. Instead, the unimorph cantilever beam consists of only one layer of piezoelectric material and one layer of substrate layer (Fig. 1).

In this paper, we use a simple bimorph beam with a tip mass on its open end. We replace the material of the tip mass and the substrate layer of the beam evaluate the difference of outcome on the use of different materials. We also change the size of the tip mass to vary its weight to inspect the difference in the power generation outcome. Additionally, we set these tip masses in three different locations of the beam keeping the size of the tip mass constant. We scrutinize the data obtained from placing these tip masses from closest to furthest from the fixed end of the beam to propose a valid conclusion.

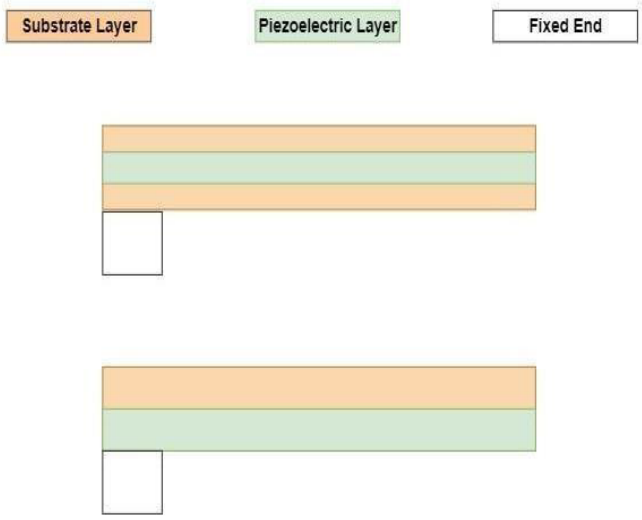

Fig. 1. Bimorph and Unimorph cantilever beam set-up.

2. Method

2.1. Analytical model

Newton's second law of motion can be used to derive an equation of motion for a single cantilever beamed piezoelectric energy harvester,

$$m\frac{d^2x}{dt^2} = -kx(t) + F(t) \quad (1)$$

In the circumstance above, m indicates the mass of the cantilever beam, k is the stiffness of the cantilever beam; x(t) and F(t) signifies the displacement of the beam as a function of time and the applied force on the cantilever beam. In the context of equation (1), the left-hand side corresponds to the internal force whereas the right side of the equation accounts for the restoring force of the beam and the external force applied on the beam.

Subsequently, Eq. (2) accounts for the piezoelectric effect caused by the piezoelectric material to relate the generated charge by the piezoelectric material and the mechanical deformation.

$$q(t) = d\,.\,p(t) \tag{2}$$

In the context of Eq. (2), q(t) is the charge generated, p(t) stands for the mechanical deformation of the piezoelectric material and d is the piezoelectric charge coefficient. The generated charge related to the voltage generation as per Eq. (3),

$$V(t) = -\frac{q(t)}{C} \tag{3}$$

In this scenario, V(t) denotes the generated voltage and according to equation, the generation of voltage depends on C, which stands for the capacitance of the harvester. The capacitance depends on the dimension of the harvester and can be expressed by,

$$C = \frac{2\varepsilon b L_p}{h_p} \tag{4}$$

In Eq. (4), ε is the dielectric constant, b symbolizes the width of the cantilever beam, Lp and h_p are the piezoelectric length and the width of the piezo layer.

This analytical model has been implemented in COMSOL Multiphysics to generate voltage and electrical output in a frequency domain by changing the configuration of the system based on the changes made with the substrate layer and the tip mass placed on top of the beam in various locations of the beam.

2.2. Selection and design of the cantilever beam

The process of converting vibration energy into electric power involves two steps. First, the conversion of mechanical energy is achieved by using a converter to translate the vibrations into relative motion between two mechanical components. Next, the converted mechanical energy is further transformed into electrical energy by utilizing mechanical-to-electrical converters, such as piezoelectric materials or variable capacitors [14]. Out of the three methods for harvesting energy, namely electromagnetic, electrostatic, and piezoelectric techniques, the piezoelectric approach is the most popular and commonly used. This is because it is capable of harvesting vibration energy over a wide range of frequencies, and it has a simple design that is easy to create. Additionally, the piezoelectric energy harvester is efficient in converting energy and allows real-time monitoring, making it a better option than the other available methods [15-17]. Regarding the configuration of the beam, bimorph set-up was selected. Since the purpose of the study is the enhancement of the outcome, bimorph cantilever structure has been adapted since it doubles the energy capacity without significantly increasing the unit volume [18].

To obtain meaningful results from the simulation, several different configurations of the bimorph cantilever beam were created in COMSOL Multiphysics. This was achieved by altering placement of the tip mass and experimenting with various substrate materials. The built in COMSOL design for bimorph cantilever beam was used [19] and then further implications were done by changing the selected substrate materials from the Built-in library and by changing the dimensions of the proof mass and its location on the beam. Numerous parameters have been defined, each dependent on the specific variations introduced in the setup These parameters play a crucial role helping in understanding how changes in the setup affect the performance of the system. In [19], only structural steel has been used within a frequency range of 62-80 Hz. Structural steel is one of the materials we have used for the experimentation, and the obtained results are identical to [19], as shown in Fig. 2. Hence, the results achieved by using other materials from the built-in material library of COMSOL Multiphysics validate the results.

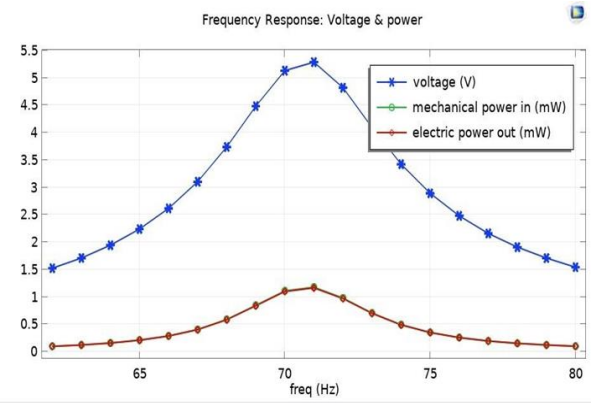

Fig. 2. Validation of obtained results.

The simulation of piezoelectric cantilever beam involved utilizing the parameters listed in Table 1. The study considered seven different materials for the substrate layer to explore variations in the configurations. It is important to note that the piezoelectric layer remained consistent and was defined as PZT-5A material throughout the simulations. The material properties of both the piezoelectric layer and the various substrate materials were pre-defined in COMSOL Multiphysics, ensuring their constant values, and no additional user-defined parameters were necessary. The built-in material properties in COMSOL Multiphysics facilitated the simulation process and enabled the evaluation of the different configurations effectively.

Table 1. Parameter of the piezoelectric cantilever beam.

Parameters	Value
Type of Beam	Bimorph
Piezoelectric layer material	Lead Zirconate Titanate (PZT-5A)
Substrate layer material	Several
Tip mass material	Several
Length of the beam	21 mm
Height of the beam	0.16 mm
Thickness of piezoelectric layer	0.06 mm/ each
Thickness of substrate layer	0.04 mm

During the operational phase, the parameters of the cantilever beam remained fixed, and a tip mass was affixed to its free end. To investigate the influence of the tip mass on the system's frequency response, its position and dimensions were systematically modified. Fig. 3 visually presents the various configurations of the tip mass situated on top of the cantilever beam. The specific sizes and positions of the tip mass corresponding to configurations A, B, C, D and E in Fig. 3 are detailed in Table 2. This analysis aimed to understand how different tip mass setups affect the dynamic behaviour of its system's frequency response.

Configuration C, D and E use the same dimension of tip mass; however, these tip masses were placed in different locations of the cantilever beam. Configuration D and E are the same as configuration C, except for one variable which is the distance of the tip mass from the fixed end of the cantilever beam that has been changed.

Table 2. Parameters of different configurations.

Parameters of tip mass	**A**	**B**	**C**	**D**	**E**
Width (mm)	4	4	2	4	2
Height (mm)	5.7	1.7	1.7	1.7	1.7
Distance from the host structure (mm)	15.75	15.75	15.75	17.75	13.75

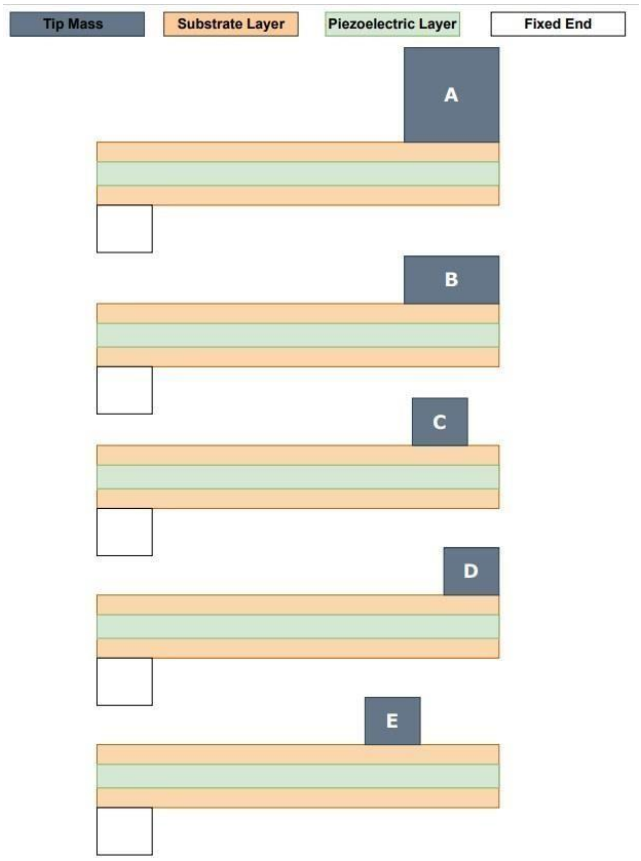

Fig. 3. Different configuration of the cantilever beam.

2.3. Simulation

In the design and simulation of piezoelectric energy harvesting system, COMSOL Multiphysics served as the primary software for drawing and evaluating the system's performance. A 2D model of the cantilever beam was created, incorporating the parameters specified in Table 1. The setup involved a fixed host structure at one end of the beam, while the size, shape, location, and presence of the tip mass at the other free end were varied as shown in Fig. 3. The changes in tip mass parameters corresponding to configurations A, B, C, D, and E are accurately detailed in Table 2. Additionally, Table 3 provides an overview of the material properties used from the built-in material library within COMSOL Multiphysics. This comprehensive approach allowed for an in-depth analysis of the piezoelectric energy harvesting system and its behaviour under different tip mass configurations.

Table 3. Properties of the used materials.

Material	Young's Modulus (Pa)	Density (kg/m^3)	Poisson's ratio
Lead Zirconate Titanate (PZT-5A)	66×10^9	7750	0.31
Structural Steel (SS)	200×10^9	7850	0.30
Aluminum (Al)	70×10^9	2700	0.33
Cast Iron (Ci)	140×10^9	7000	0.25
Copper (Cu)	110×10^9	8960	0.35
Tungsten (W)	411×10^9	19350	0.28
Lead (Pb)	16×10^9	11340	0.44
Nickel (Ni)	219×10^9	8900	0.31

In the simulation process, various boundary conditions were applied to the cantilever beam to explore different potential outcomes. For instance, a mechanical damping value of 0.001 was set at the hinged end of the beam to account for damping effects. On the other hand of the beam, free boundary conditions were maintained, allowing displacement in response to vibrations. These boundary conditions remained consistent for all the different cases studied in this research. The frequency range for the simulations was set between 0 Hz to 300 Hz, considering the typical frequency range of various piezoelectric products and their applications [20]. This range was chosen to comprehensively assess the behaviour of the piezoelectric energy harvesting system over a relevant frequency spectrum. By applying these boundary conditions and frequency range, the study aimed to analyse and optimize the system's performance under diverse scenarios.

3. Results and Discussion

In the resultant frequency response curves, the performance of each configuration was analysed in terms of voltage and power. Both the voltage and power frequency curves showed similar pattern throughout the simulation. Therefore, only the voltage output graphs will be extracted for this paper. However, both voltage and power output will be discussed accordingly for all cases. It was observed that the piezoelectric material which resonated first in the spectrum of the frequency in Tungsten, followed by lead, copper, nickel, structural steel, cast iron and aluminium.

3.1. Case A

Figure 4 shows that there were four harmonic responses generated by the energy harvesting system at frequency beyond 200 Hz which was produced by Tungsten, lead, copper, and nickel material. The peak voltage output produced by these harmonic peaks of each material are very low compared to their first peak. Hence, only the first peak shall be taken into consideration to harvest energy. The first peak is noticed at 25 Hz achieved by tungsten with a high voltage and power output of 25.72 V and 27.57 mW respectively. The rest of the materials have followed the pattern mentioned earlier, where lead being the second to resonate at 31 Hz with a magnitude of 17.93 V and 13.405 mW and aluminium being the last to resonate at 64 Hz with the lowest output among all, 5.6V and 1.32 mW. Copper, nickel, structural steel and cast iron resonate at 36 Hz, 37 Hz, and 41 Hz respectively. In almost every case, the peak output at any frequency has a major difference between the previous and the immediate next frequency. Tungsten for example, if we compare the outputs at 24 Hz and 26 Hz with its resonance frequency, a clear remark can be drawn of the problem statement. However, aluminium has been able to keep the difference between the outputs near to its resonance frequency rather minimum.

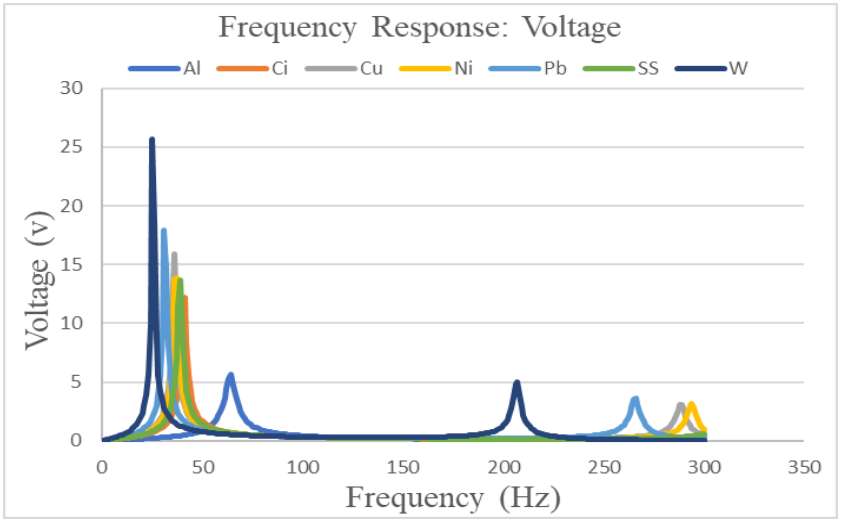

Fig. 4. Frequency response graph for case A.

Table 4 illustrates a comparison of output voltage of different materials for frequencies near to the resonance frequency, where N represent the resonance frequency of the respective material. The subsequent frequency which differs by 1 Hz is denoted as N+1 and N-1 respectively. N is the resonance frequency, as the table clarifies that although almost every material is producing a high voltage output, the output near to N is not stable. In fact, N-1 and N+1 point out how significant the difference is. The rise from N-1 to N is sharp, compared to the decline curve from N to N+1, where this is only applicable for the heavier materials such as tungsten, lead, copper. However, for materials such as nickel, structural steel, and cast iron the uprising curve is less stiff than the declining curve. The only exception is aluminium. Although aluminium produces the lowest output amongst the materials, the output around the peak resonance is marginal.

Table 4. Output voltage for different material in the intervals of its resonance frequency for Case A.

Material	N-2	N-1	N	N+1	N+2
Tungsten (W)	5.69	9.96	25.72	18.48	8.68
Lead (Pb)	5.60	9.19	17.93	14.73	8.05
Copper (Cu)	6.60	11.03	15.86	10.25	6.43
Nickel (Ni)	8.02	13.7	13.90	8.27	5.53
Structural steel (SS)	6.96	11.33	13.66	8.89	5.85
Cast iron (Ci)	6.94	10.81	12.25	8.32	5.65
Aluminium (Al)	4.49	5.31	5.63	5.12	4.28

3.2. Case B

The simulated results obtained through simulation of Case B is as shown in Fig. 5. The materials have shown results in same order, tungsten being the first one to peak with the highest voltage and power output and aluminium being the last and having the least efficient outcome. Tungsten's first peak is at its resonance frequency of 47 Hz, with voltage and power outputs of 11.7 V and 5.28 mW respectively. Similarly, lead produces voltage and power output of 7.01 V and 2.05 mW at its resonance frequency of 58 Hz. Copper and nickel dictate at 66 Hz and 67 Hz, with an output of 5.859 V, 1.43 mW and 5.851 V, 1.42 mW respectively. Aluminium gives the lowest output among all the materials, peaking at 111 Hz with 2.63 V and 0.28 mW. Steel and cast iron delivered 5.28 V, 1.16 mW and 4.8 V, 0.989 mW at 71 Hz and 74 Hz.

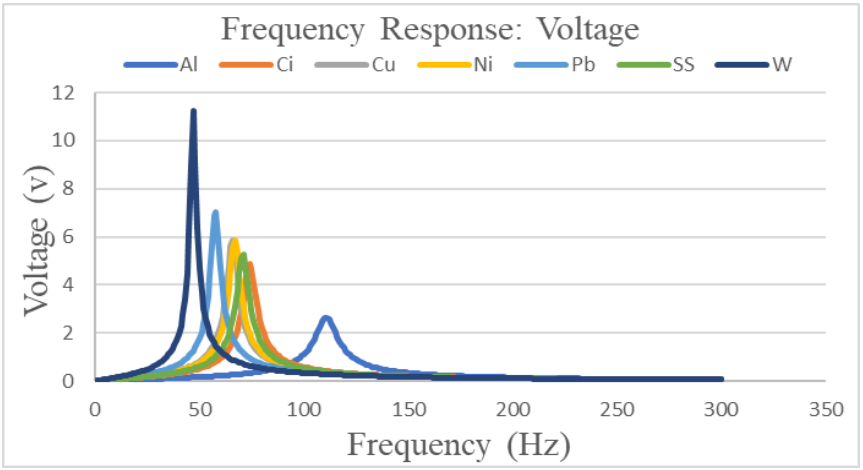

Fig. 5. Frequency response graph for case B.

In comparison with the frequency response with case A, the peak voltage at the resonance frequency for all materials decreased to be at least 50% lower in case B. The resonant frequency of each piezoelectric beam is also shifted and increased by 50% in comparison with the configurations applied in case A. Most importantly, the graphs produced by Case B are curvier than Case A. Hence, the sudden spike from one frequency to the next is less prominent in case B.

Table 5 illustrates a comparison of output voltage of different materials for frequencies near to the resonance frequency for case B. The problem of unstable

peak outputs is absent in case B. In Case A, only aluminium produced outputs near the resonance frequency that are stable. However, in this case, except for tungsten and lead, all the other materials have projected outputs whose magnitudes are similar to the magnitude achieved at N. Most of the materials produced similar results at N-1 and N+1, whilst aluminium displayed stability even at N-2 and N+2.

Table 5. Output voltage for different material in the intervals of its resonance frequency for Case B.

Material	N-2	N-1	N	N+1	N+2
Tungsten (W)	6.15	8.93	11.26	9.07	6.33
Lead (Pb)	5.63	6.87	7.01	5.92	4.68
Copper (Cu)	4.79	5.63	5.85	5.26	4.38
Nickel (Ni)	4.68	5.54	5.85	5.33	4.45
Structural steel (SS)	4.48	5.13	5.28	4.82	4.09
Cast iron (Ci)	4.03	4.61	4.87	4.61	4.03
Aluminium (Al)	2.49	2.61	2.63	2.56	2.41

3.3. Case C

Figure 6 illustrates the frequency response output obtained in the simulation of case C energy harvesting system. It is shown that tungsten resonates at 70 Hz with an outcome of 6.3 V, 1.65 mW and aluminium resonate at 147 Hz resulting in 2.02 V, 0.17 mW. Lead, copper, nickel, structural steel and cast iron remain in the middle topping at 95 Hz (3.66 V, 0.56 mW), 97 Hz (3.64V, 0.55 mW), 102 Hz (3.37 V, 0.47 mW) and 106 Hz (3.15 V, 0.41 mW) respectively. Case A, B and C are similar, having the same distance from the hinged end of the cantilever beam, however, the only difference is the size of the tip mass, more specifically the weight of the tip mass. Compared to case A and B, case C has the lightest tip mass while Case A has the heaviest. Comparing the results among these three cases it was observed that the change in the weight of the tip mass results in the alteration of its resonance frequency and voltage output.

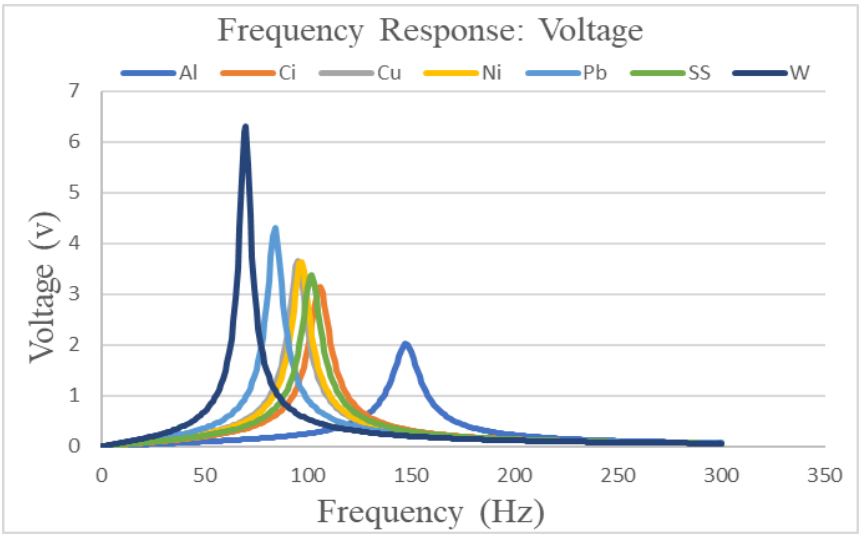

Fig. 6. Frequency response graph for case C.

Table 6. Comparison of results for Case A, Case B and Case C.

Material	Frequency (Hz)			Voltage (V)		
	Case A	Case B	Case C	Case A	Case B	Case C
Tungsten (W)	25	47	70	25.72	11.26	6.30
Lead (Pb)	31	58	84	17.93	7.01	4.30
Copper (Cu)	36	66	95	15.86	5.85	3.66
Nickel (Ni)	37	67	97	13.90	5.85	3.64
Structural Steel (SS)	39	71	102	13.66	5.28	3.37
Cast Iron (Ci)	41	74	106	12.25	4.87	3.15
Aluminium (Al)	64	111	147	5.63	2.63	2.02

In case A, where the tip mass is the heaviest, all the materials have reached their resonance frequency early in the range. In fact, four of the materials have even shown a harmonic frequency. The output voltages obtained in case A are also way higher compared to the other two cases. Whereas, in case C, where the tip mass is the lightest, the resonance has occurred further in the range and the achieved results do not hold magnitudes as significant as the previous two cases. Hence, the results established the fact that upon placing in the same location and maintaining the same distance from the fixed point of the cantilever beam, the energy harvesting system with heavier the tip mass is able to produce higher output at a lower frequency and vice versa.

This is also applicable for the change of materials. Each of the materials has the same dimensions in every case. However, some of the materials are heavier than the others. Since the dimensions of the tip masses used in each case and the density of each material are known, the mass and the weight of the tip mass can be calculated.

For example, in case A, the known variables are used to identify the mass of the tip mass and for different materials.

Given that the height, weight, and length of the mass is 1 mm, 4 mm and 5.7 mm, the volume of the tip mass can be calculated using equation (5)

$$Volume = height\ x\ width\ x\ length = 2.28\ x\ 10^{-8}\ \text{m}^3 \tag{5}$$

$$Density = \frac{Mass}{Volume} \tag{6}$$

Subsequently, the mass for each different material for tip mass can be determined by re-writing equation (7)

$$Mass = Volume\ x\ Density \tag{7}$$

Table 7 shows the calculated mass for each of the materials applied in the tip mass for Case A, Case B and Case C.

Table 7. Calculated mass of the tip mass for different materials in Case A, Case B and Case C.

Material	Mass (g)		
	Case A	Case B	Case C
Tungsten (W)	0.441	0.131	0.066
Lead (Pb)	0.258	0.077	0.038
Copper (Cu)	0.204	0.061	0.030
Nickel (Ni)	0.202	0.060	0.030
Structural Steel (SS)	0.178	0.053	0.027
Cast Iron (Ci)	0.159	0.047	0.023
Aluminium (Al)	0.061	0.018	0.009

Using the results obtained in Table 6 and 7, it is found that the mass contributes to the change of voltage and power output as the other variables are kept constant. Hence, if any application requires a small size of tip mass without sacrificing the optimum output, these are the cases when heavier materials such as tungsten or lead can be used to satisfy the circumstances.

3.4. Case D

As aforementioned in 2.2, Case D and Case E are the continuation of Case C by using different locations of the tip mass on the cantilever beam. For Case D, the tip mass is pushed further to the free end of the cantilever beam while for Case E, the tip mass is placed closer from the fixed end of the beam. The results extracted for case D are close to the results obtained in case C, however, the resonance appears to be in a lower frequency in this case.

Figure 7 shows the frequency response curves for each material applied in Case D. Each of the materials has shown their peak at a lower frequency compared to Case C, with higher output voltages.

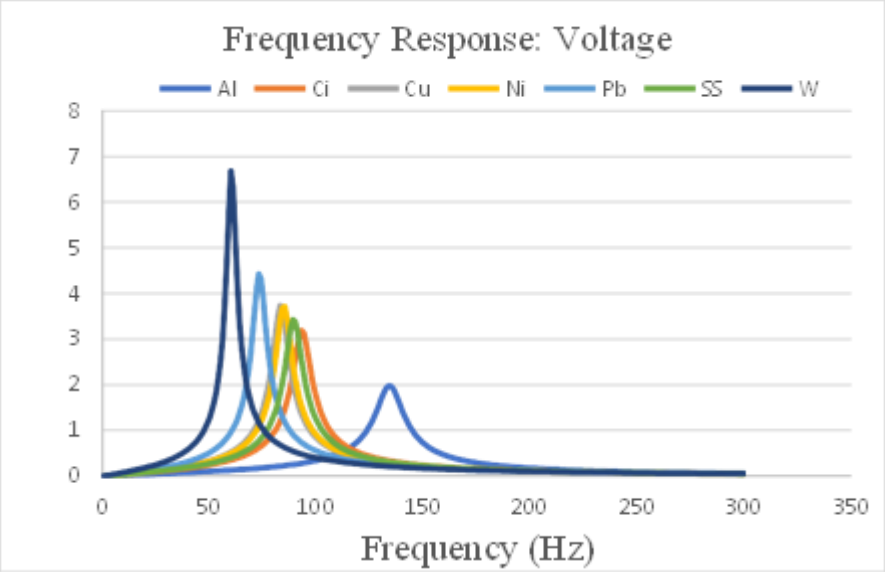

Fig. 7. Frequency and voltage response for case D.

3.5. Case E

The frequency response output for Case E is simulated and shown in Fig. 8. The materials resonate in a higher frequency and marginally lesser magnitude in values in case E compared to case C. The first resonance occurs at 82 Hz and the last at 162 Hz which is quite a big margin of difference for a small margin of difference in the outcome. Table 8 provides a comparison for the output of different locations of tip mass for Case C, Case D and Case E to highlight the impact in the selection of placement for tip mass on the cantilever beam.

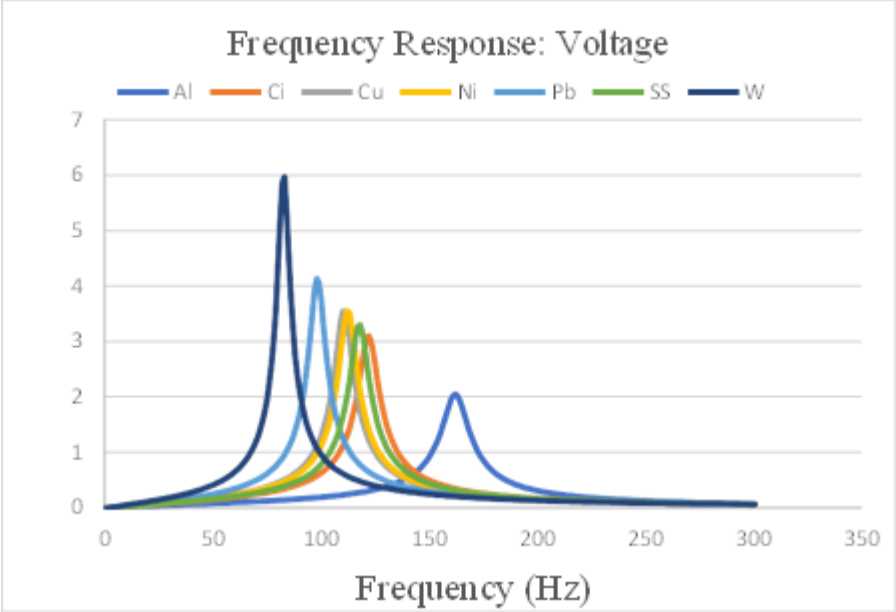

Fig. 8. Frequency and voltage response for case E.

Table 8. Comparison of Results for Case C, Case D and Case E.

Material	Frequency (Hz)			Voltage (V)		
	C	D	E	C	D	E
Tungsten (W)	70	60	82	6.30	6.69	5.97
Lead (Pb)	84	73	97	4.30	4.33	4.13
Copper (Cu)	95	83	109	3.66	3.74	3.55
Nickel (Ni)	97	85	111	3.64	3.72	3.55
Structural Steel (SS)	102	89	117	3.37	3.43	3.30
Cast Iron (Ci)	106	93	121	3.15	3.19	3.10
Aluminium (Al)	147	134	162	2.02	1.98	2.05

Unlike the first three situations, for Case C, Case D and Case E all the tip masses hold the same mass as displayed in Table 7 (Same as C), which leads to conclude that the position of the tip mass on top of the beam holds effect on the overall outcome. As mentioned earlier, and upon the scrutiny of data presented in Table 8, it is established that the further the tip mass is positioned on the beam, the higher the output value (both voltage and power) at a lower frequency. However, only aluminium displays lower value when the mass is placed further on the beam

4. Conclusion

This paper investigates the effect of tip mass on the voltage and power output of the piezoelectric energy harvesting system in terms of its materials, dimensions, and location on the cantilever beam. The results obtained by changing the dimensions of the tip mass and using different materials as the tip mass is evident that a heavier material can produce better results. Furthermore, this paper clearly establishes that the location of the tip mass on the cantilever beam affects the voltage and power output of the energy harvesting system. The combined knowledge of the effect of the mass and the position of the tip mass open doors to

many applications and devices. Furthermore, the validation of the length-width ratio of the cantilever beam affecting the frequency response output proven by [21] may be an addition to the overall idea of enhancing the magnitudes of voltage or power outcome for a wide range of devices or applications [22, 23]. Above all, this paper discusses the simplest way of generating maximum results. There are many proposed techniques and methods to enhance the outcome such as frequency tuning and magnetic coupling, but this paper discusses the simplest method of producing different outcomes from a single model by differing the materials and the position of the tip mass. This fundamental knowledge of the effect of the tip mass's location and weight can be implemented to model a multiple beam energy harvester to generate a broadband output.

Acknowledgements

This work was supported by the Ministry of Higher Education of Malaysia under the Fundamental Research Grant Scheme (FRGS/1/2020/TK0/MMU/03/13). The authors would also like to acknowledge the Faculty of Engineering and Technology, Multimedia University for the support given in conducting this research.

References

1. Ahmed, R.; Mir, F.; and Banerjee, S. (2017). A review on energy harvesting approaches for renewable energies from ambient vibrations and acoustic waves using piezoelectricity. *Smart Materials and Structures, 26*(8), 085031.
2. Chen, J.; Qiu, Q.; Han, Y.; and Lau, D. (2019). Piezoelectric materials for sustainable building structures: Fundamentals and applications. *Renewable and Sustainable Energy Reviews, 101*, 14-25.
3. Mohanty, A.; Parida, S.; Behera, R. K.; and Roy, T. (2019). Vibration energy harvesting: A review. *Journal of Advanced Dielectrics, 9*(4), 1-17.
4. Wang, H.; and Meng, Q. (2013). Analytical modelling and experimental verification of vibration-based piezoelectric bimorph beam with a tip-mass for power harvesting. *Mechanical Systems and Signal Processing, 36*(1), 193-209.
5. Tang, L.; and Wang, J. (2017). Size effect of tip mass on performance of cantilevered piezoelectric energy harvester with a dynamic magnifier. *Acta Mechanica, 228*(11), 3997-4015.
6. Shindo, Y.; and Narita, F. (2014). Dynamic bending/torsion and output power of S-shaped piezoelectric energy harvesters. *International Journal of Mechanics and Materials in Design, 10*(3), 305-311.
7. Zhou, W.; Penamalli, G.R.; and Zuo, L. (2012). An efficient vibration energy harvester with a multi-mode dynamic magnifier. *Smart Materials and Structures, 21*(1), 015014.
8. Aldraihem, O.; and Baz, A. (2011). Energy harvester with a dynamic magnifier. *Journal of Intelligent Material Systems and Structures, 22*(6), 521-530.
9. Aladwani, A.; Aldraihem, O.; and Baz, A. (2014). A distributed parameter cantilevered piezoelectric energy harvester with a dynamic magnifier. *Mech. Mechanics of Advanced Materials and Structures, 21*(7), 566-578.
10. Kouritem, S.A.; Al-Moghazy, M.A.; Noori, M.; and Altabey, W.A. (2022). Mass tuning technique for a broadband piezoelectric energy harvester array. *Mechanical Systems and Signal Processing, 181*, 109500.

11. Mohamed, K.; Elgamal, H.; and Kouritem, S.A. (2021). An experimental validation of a new shape optimization technique for piezoelectric harvesting cantilever beams. *Alexandria Engineering Journal*, *60*(1), 1751-1766.
12. Shin, Y.-H.; Choi, J.; Kim, S.J.; Kim, S.; Maurya, D.; Sung, T.-H.; Priya, S.; Kang, C.-Y.; and Song, H.-C. (2020). Automatic resonance tuning mechanism for ultra-wide bandwidth mechanical energy harvesting. *Nano Energy*, *77*, 104986.
13. Shenck, N.S.; and Paradiso, J.A. (2001). Energy scavenging with shoe-mounted piezoelectrics'. *IEEE Micro, 21(3)*, 30-42.
14. Ghosh, S.K.; and Mandal, D. (2017). Sustainable energy generation from piezoelectric biomaterial for noninvasive physiological signal monitoring. *ACS Sustainable Chemistry & Engineering*, *5*(10), 8836-8843.
15. Minghui, Y.; Li, M. A.; and Wei, Z. (2018). Study on power generations and dynamic responses of the bistable straight beam and the bistable L-shaped beam. *Science China Technological Sciences*, 61, 1404-1416.
16. Karami, A.; Galayko, Di.; and Basset, P. (2017). A novel characterization method for accurate lumped parameter modelling of electret electrostatic vibration energy harvesters. *IEEE Electron Device Letters, 38*(5), 665-668.
17. Pei, Y.; Liu, Y.; and Zuo, L. (2018). Multi-resonant electromagnetic shunt in base isolation for vibration damping and energy harvesting. *Journal of Sound and Vibration, 423*, 1-17.
18. Thein, C.K.; Ooi, B.L.; Liu, J.S.; and Gilbert, J.M. (2016). Modelling and optimisation of a bimorph piezoelectric cantilever beam in an energy harvesting application. *Journal of Engineering Science and Technology, 11*(2), 212-227.
19. Malkin, M.C.; and Davis, C.L. (2005). Multi-frequency piezoelectric energy harvester. *The Journal of the Acoustical Society of America*, *118*(1), 24.
20. Malaji, P.V.; and Ali, S.F. (2015). Analysis of energy harvesting from multiple pendulums with and without mechanical coupling. *The European Physical Journal Special Topics, 224*(14-15), 2823-2838.
21. Tong, W.P.Q.; Muhammad Ramadan, B.M.S.; and Logenthiran, T. (2018). Design and simulation of a piezoelectric cantilever beam for mechanical vibration energy harvesting. *Proceedings of the 2018 IEEE Innovative Smart Grid Technologies - Asia (ISGT Asia)*, Singapore, 1245-1250.
22. Pertin, O.; Shrivas, P.; Guha, K.; Rao, K. S.; and Iannacci, J. (2021). New and efficient design of multimode piezoelectric vibration energy harvester for MEMS application. *Microsystem Technologies, 27*(9), 3523-3531.
23. Piyarathna, I.E.; Lim, Y.Y.; Edla, M.; Thabet, A.M.; Ucgul, M.; and Lemckert, C. (2023). Enhancing the bandwidth and energy production of piezoelectric energy harvester using novel multimode bent branched beam design for human motion application. *Sensors*, 23(3), 1372